



Stockholm  
University

# Bachelor Thesis

Degree Project in  
Geochemistry 15 hp

**Reconstructing changes in atmospheric mineral dust and  
effective humidity during the last 5400 cal yr BP using  
geochemical proxies from Davidsmosse, SW Sweden**

Anna Virolainen



Stockholm 2016

Department of Geological Sciences  
Stockholm University  
SE-106 91 Stockholm  
Sweden

# Reconstructing changes in atmospheric mineral dust and effective humidity during the last 5400 cal yr BP using geochemical proxies from Davidsmosse, SW Sweden

Anna Virolainen

2016-01-29

## Abstract

Ombrotrophic peat bogs has the potential of providing high-resolution paleorecords of terrestrial deposition of atmospheric dust, an important climate controller. However, relatively few paleodust records have been compiled from peat and thus mineral dust is less studied than the botanical, organic and chemical properties in raised bogs. Here, a multiproxy approach was applied to infer changes in dust deposition and effective humidity in southwest Sweden during the last 5400 cal yr BP using a peat sequence from Davidsmosse (N56°59'10.15", E13°00'32.60"). Elemental profiles were studied together with bulk density, ash content, C/N ratio and stable isotope data of  $\delta^{13}\text{C}$  to reconstruct dust events and general trends in humidity. Elemental data (Al, Si, P, K, Ca, Ti, Fe, Zn, Br, Rb, Sr, Pb, Zr and Y) was acquired using two different X-ray fluorescence (XRF) methods: a conventional WD-XRF to analyse bulk elemental composition and an XRF core scanner, to analyse the elemental composition of ashed peat. Comparison of the results from the two methods showed generally good correlation between the elemental variations retrieved. The results suggest that XRF-CS on ashed peat is an applicable method for inferring relative changes in dust related elements. Furthermore, this study has identified six possible periods of elevated dust deposition since mid-Holocene: 4440-4250, 3600-3300, 3250-3100, 2900, 2400-2200 and 1500-1200 cal yr BP. The earliest and the two latest dust events correspond to events found in the dust record compiled by Kylander *et al.* (2013) from Store Mosse. Agreement in time between these period of elevated dust found in two ombrotrophic bogs located 60 km apart, suggest that the dust events were of regional scale. Additionally, three periods of predominantly wetter conditions (4300-3650, 2700-2300 and 1600-1300 cal yr BP) and three periods of drier conditions (3600-2700, 2250-1700 and 1300-present) were interpreted from the multi proxy record retrieved from Davidsmosse. The humidity shifts occur in good agreement with the dust events.

KEYWORDS: mineral dust, XRF, ombrotrophic peat, humidity, Holocene

---

## 1. Introduction

Ombrotrophic peat bogs only receive input from the atmosphere and can therefore act as archives of past dust deposition and climate. Paleodust reconstructions are of interest as atmospheric mineral dust affect Earth's climate system by interacting with radiation, cloud formation, biogeochemical cycles and transporting nutrients to terrestrial and marine systems (Kohfeld and Harrison, 2001). As the main part of dust transported by the atmosphere is estimated to be deposited on land (Shao *et al.*, 2011) terrestrial archives such as peat are important records for determining past variations in dust.

Peat is a relatively easily accessible and high resolution record that has been used for environmental reconstruction since the late 19<sup>th</sup> and early 20<sup>th</sup> century. Blytt (1876, 1882) and Sernander (1908) performed peat stratigraphy in northern Europe and connected changes in the stratigraphy to changes in climate. Since then ombrotrophic bogs have been used for analyses of for example atmospheric lead deposition and pollution (e.g. Klaminder, *et al.* 2003; Martínez Cortizas *et al.*, 2012), peat properties

connected to climate (e.g. Kuhry and Vitt, 1996; Hansson *et al.*, 2013; Loisel *et al.*, 2015) and minerogenic content and geochemistry (e.g. Tolonen, 1984; Muller *et al.*, 2008; Margalef *et al.*, 2014).

*Sphagnum* dominated bogs are good archives of atmospheric deposition as the branched structure of the mosses captures particulate matter and the high cation exchange capacity allows the mosses to retain dissolved metals (De la Rosa *et al.*, 2003). Bogs are, however, nutrient limited systems so not all elements deposited on the bog surface can be assumed to be preserved in the peat record. *Sphagnum* dominated bogs usually have acidic pH so mineral dust sensitive to acidic conditions may dissolve and elements that are essential nutrients may be recycled by plants. Furthermore, as peatlands are waterlogged areas with fluctuating water table, redox sensitive elements may act mobile in the record. This leaves the biogeochemically conservative elements being the main constituents preserved of the atmospheric dust signal.

Mineral dust deposited in an ombrotrophic bog was used by De Jong *et al.* (2006) to reconstruct past storminess in southwest Sweden. However, the first dust record compiled from a raised bog in Sweden using conservative elemental geochemistry was performed by Kylander *et al.* (2013) on a peat sequence retrieved from Store Mosse, southcentral Sweden. A second study by Kylander *et al.* (in review) on the same sequence has focused on characterising changes in the mineral deposition. Together the two studies summarise the paleoenvironmental development of mineral dust deposition and effective humidity in southcentral Sweden and four distinct dust events have been identified after 8900 cal yr BP. The purpose of this BSc project has been to compile a dust record of another ombrotrophic peat bog in Sweden, Davidsmosse, for comparison with the record from Store Mosse.

The site Davidsmosse is part of a wider project on dust deposition in southern Sweden and some basic information on the sequence was available at the start of this Bsc project. Fieldwork and coring, subsampling and freeze-drying, carbon and nitrogen analyses, <sup>14</sup>C-dating and age modelling was carried out by a team of collaborators as described below (Table 1.). The previously acquired information was used as a compliment to the data generated during this project. The methods used here have focused on geochemical analyses of the mineral dust incorporated in the peat record. Variation of selected major (Al, Si, P, K, Ca, Ti and Fe) and trace elements (Zn, Br, Rb, Sr, Y, Zr and Pb) were determined using two X-ray fluorescence (XRF) methods. An analytical aspect to the project was to compare the two methods in order to evaluate XRF core scanning (XRF-CS) on ashed peats to the more conventional wavelength dispersive XRF (WD-XRF) on bulk peat. Finally, the elemental data was combined with geochemical and physical proxies to reconstruct changes in mineral dust deposition and effective humidity (wet/dry) during the last 5400 years.

### 1.1. Objectives and aim

The aim of this project was to reconstruct changes in paleoenvironmental conditions in southwest Sweden over the last 5400 cal yr BP in regard to dust deposition and general trends in humidity. The specific objectives have been to (i) compare the results from WD-XRF on bulk peat and XRF-CS on ashed peats and (ii) reconstruct changes in mineral dust deposition and effective humidity.

**Table 1** Compilation of work previously done on the peat samples from Davidsmosse.

| Previous work performed on the cores           |  |
|--|--|
| Sampling and field work                        | Dr. Malin Kylander, Prof. Richard Bindler, Prof. Antonio Martínez Coritaz & Dr. Sophia Hansson |
| Subsampling and freeze drying                  | Dr. Sophia Hansson   |
| Carbon and nitrogen analyses                   | Dr. Sophia Hansson   |
| <sup>14</sup> C-dating and age-depth modelling | PhD student Jenny Sjögren  |

## 2. Method and materials

### 2.1 Site description and sampling

Davidsmosse is an ombrotrophic peat bog located in Halland, southwest Sweden. The bog is located approximately 60 km southwest of Store Mosse, which is a large mire complex in the boreal-nemoral zone in southern Sweden subjected to several previous studies (e.g. Svensson, 1988; Hansson *et al.*, 2013; Kylander *et al.*, 2013; Kylander *et al.*, in review). At Davidsmosse 5 m of peat equals accumulation during the last 5400 cal yr BP, which can be compared with Store Mosse where 5.5m of peat accumulation corresponds to the last 8900 years (Kylander *et al.*, in review). Davidsmosse is thus a high-resolution peat record with each cm representing approximately 11 years. There are signs of modern drainage on the northern end of the bog, however, drainage does not appear to have lowered the water table significantly below the acrotelm and the main part of the peat record appears to be preserved. *Sphagnum* mosses dominate but *Carex* ssp. and smaller pine trees are present as well.

In May 2014 cores were recovered from the domed Davidsmosse (N56°59'10.15'', E13°00'32.60'') using a Russian corer (diameter 7.5 cm). Seven overlapping 1 m sections were taken in two adjacent parallel holes to a depth of 498 cm. The cores were frozen prior to sub-sampling in contiguous 1 cm slices using a stainless steel saw and then freeze-dried.

### 2.2. Age model, carbon and nitrogen analyses

A total of 6 <sup>14</sup>C-dates were made at Tandemlaboratoriet, Uppsala University and at BETA analytical Inc., London, UK. The Clam program version 2.2. (Blaauw, 2010) was used for age-depth modelling (Fig. 1). The program includes calibration of the <sup>14</sup>C-dates and the calibration curve IntCal-13 (Reimer *et al.*, 2013) was used. The data was modelled applying a smooth spline interpolation and updated using true depths (section 2.3.).

Analyses of total carbon, nitrogen and  $\delta^{13}\text{C}$  were performed at 5 cm resolution.

### 2.3. Bulk density, true depth and ash content

Bulk density ( $\text{g}/\text{cm}^3$ ) was calculated by dividing the dry weight of a sample by its estimated volume ( $\pm 10\%$ ). True depths of the subsamples, adjusted for irregularities in the coring, were determined via alignment of the bulk density profiles of the cores. Photographs of the “fresh” cores were also used to visually assess the alignment. In total the core sections covered a depth of 498cm, though the top 30 cm of the bog was never retrieved. The true depth was used in the age-model.

Dry ashing of the samples were performed at 450°C overnight and the ash content of a sample was calculated as the percentage of the dry weight at 105°C. The samples were placed in a desiccator during cooling and between measurements to keep from contamination from the surrounding and to avoid weight gain from moisture.

### 2.4. Wavelength Dispersive X-ray fluorescence spectrometry (WD-XRF)

Analyses of elemental components (Al, Si, P, K, Ca, Ti, Fe, Zn, Br, Rb, Sr and Pb) of the bulk peat were carried out using a Bruker S8-Tiger WD-XRF analyser equipped with a Rh-anticathod X-ray tube, at the Department of Ecology and Environmental Sciences, Umeå University. Measurements were performed directly on milled peat, without other pre-treatment, thereby enabling the peat samples to be reused for additional analyses. Milling was done at 30 strokes/s for 3 min using a plant mill with Teflon vials and agate milling balls. The peat samples (420-525 mg) were transferred into standard plastic

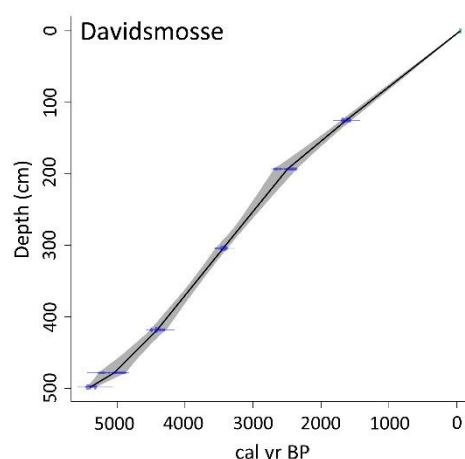


**Figure 1** Age model of the peat sequence at Davidsmosse where the depth of 498 cm equals 5393 cal yr BP.

sample cups covered with 2.5 µm Mylar® film. The measurements were performed in a low-pressure (168 mbar) helium atmosphere. Lab-ware was cleaned with ethanol between samples.

As no standard reference material (SRM) for peat was available, the analytical performance was assessed through SRM NIST-8437, hard red spring wheat flour, and by using a previously measured peat sample. Accuracy was calculated as the relative difference between the average concentration and the certified values of the SRM. Precision was calculated as the relative standard deviations of repeated measurements of the SRM and of peat samples. Precision ( $n = 9$  NIST-8437,  $n=6$  peat) was within  $\pm 10$  % (or a few ppm) for Al, Si, P, K, Ca, Ti, Fe, Zn, Br and Sr. Pb was slightly higher (11%). The Rb content was below lower level of detection (LLD) in the peat sample and below limit of qualification (LOQ) in the SRM. Accuracy for P, K, Ca, Fe and Zn was within  $\pm 10$  % (or a few ppm). The SRM only had trace amounts of Al, Si, Ti, Br, Rb, Sr and Pb, which thus were below LOQ.

A method and calibration for WD-XRF measurements on loose powder sediment samples was established by Rydberg (2014) based on 10 certified reference materials (CRM), covering a wide range of elements. A similar calibration for WD-XRF measurements of peats is currently under construction but results from Rydberg (2014) can be indicative of the analytical performance of WD-XRF on peat. The results shown therein indicate that this type of method can have accuracy and precision less than  $\pm 10$  % (or a few ppm) for all elements analysed here.

### 2.5. X-ray fluorescence core scanner (XRF-CS)

The XRF-CS analyses were carried out using an ITRAX™ core scanner at the Department of Geological Sciences, Stockholm University. The XRF-CS is a variant of the classic XRF technique allowing for measurements of elemental concentrations directly on the surface of a sediment half core. However, cores with high organic content does not always analyse well. The organic matter can cause increased scattering, resulting in poorer detection limits due to less efficient excitation of elements (Croudace *et al*, 2006). Here the XRF-CS was used to acquire elemental data (Al, Si, P, K, Ca, Ti, Fe, Zn, Br, Rb, Sr, Pb, Y and Zr) from ashed peat samples packed in specially built sample boats (Fig. 2). The cup of the sample boat is approximately 8 mm long, 2 mm wide and 2 mm deep. The analyses were performed with the XRF-CS set on voltage 30 kV, current 50 mA, step size 200 µm and measurement time of 20 seconds. Mean standard error (MSE) was generally good, below 5 for most measurements but reaching up to 30 for a few. Lab-ware was cleaned with ethanol.



Figure 2 Sample boats packed with ash prepared for XRF-CS measurements.

## 3. Result

### 3.1. Elemental variations from WD-XRF and XRF-CS

The XRF-CS data is given as peak area (pa) and is semi-quantitative in nature providing a picture of relative change in concentrations. The WD-XRF data is output in absolute concentrations given as percentages or ppm. Elemental profiles from both the WD-XRF data and the XRF-CS data were plotted with depth for Al, Si, P, K, Ca, Ti, Fe, Zn, Br, Rb, Sr and Pb (Fig. 3). Profiles of Y and Zr, only retrieved from the XRF-CS, can be seen in Fig. 4. Several of the elements behave similarly in both datasets (e.g. Si, Fe, Zn and Pb), but a few elements changed curvature in the profiles from the XRF-CS data compared to the WD-XRF (e.g. Rb, Ca and Br). Rb mostly consist of a straight line in the WD-XRF dataset as it was below LLD and it also has a few negative values, which are an artefact from the processing program of the WD-XRF. Overall, the XRF-CS data appears to be more fluctuating in its profiles than the WD-XRF data.

Bivariate correlations between the same element in the two datasets (Table 2.) emphasises which profiles kept their shape and which changed ( $p$ -values  $< 0.001$  were considered significant). Pb, Fe, Zn,

Si, Ti, Al and K had strong to fairly strong correlations (0.95-0.66). Br, Rb, P, Sr (0.5 – 0.35) and Ca (-0.25) had weak to no correlation and Ca was the only element with a negative correlation.

Correlation matrices of the relationships between elements within the datasets were constructed for both the WD-XRF data (Table 3.) and the XRF-CS data (Table 4.). Rb was removed from further analyses of the WD-XRF data due to its poor analytical quality with negative concentration values. More and stronger correlations are present in the WD-XRF data (25 correlations  $\geq 0.75$ ) compared to XRF-CS data (6  $\geq 0.75$  not counting Zr, Y; 10  $\geq 0.75$  for all elements). Especially P, Ca, K, Sr and Br appears to have lost strength in correlation between the two XRF measurements. Al, Si, Ti, Zn and Pb have kept their strong correlations, although somewhat weakened ( $r = 0.81-0.91$  for WD-XRF;  $r = 0.58-0.88$  for XRF-CS).

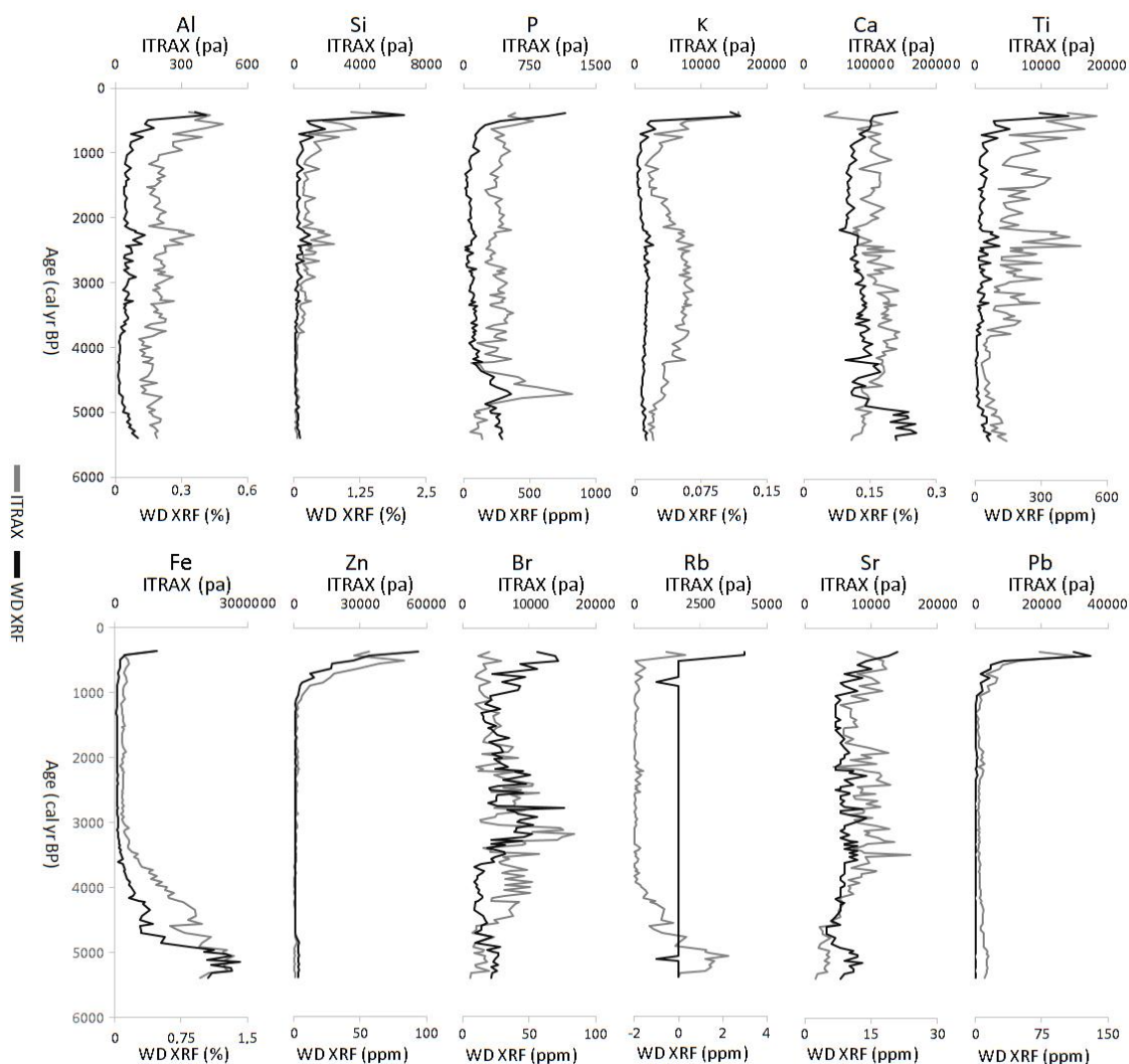


**Figure 3** Elemental profiles from the two XRF methods on bulk peat and ashed peat. The WD-XRF dataset (black) generally shows less variation than the XRF-CS dataset (grey).

**Table 2** Correlations between elemental profiles in the WD-XRF dataset and the XRF-CS dataset. The  $r$ -score is the correlation and a  $p$ -value less than 0.001 is considered significant.

|     | Al     | Si     | P    | K      | Ca    | Ti     | Fe     | Zn     | Br   | Rb   | Sr     | Pb     |
|-----|--------|--------|------|--------|-------|--------|--------|--------|------|------|--------|--------|
| $r$ | 0.69   | 0.84   | 0.19 | 0.66   | -0.25 | 0.73   | 0.91   | 0.84   | 0.05 | 0.12 | 0.35   | 0.95   |
| $P$ | <0.001 | <0.001 | 0.05 | <0.001 | 0.008 | <0.001 | <0.001 | <0.001 | 0.6  | 0.2  | <0.001 | <0.001 |

**Table 3** Correlation matrix of the elemental concentrations retrieved from WD-XRF, ash content and bulk density. Strong correlations can be seen between Al, Si, Ti, K, Zn and Pb. Good correlations are also displayed between the previous elements and P, Sr and Ash and between Ca and Fe.

|     | Al          | Si          | P           | K           | Ca          | Ti          | Fe    | Zn          | Br   | Sr   | Pb   | Ash  | BD   |
|-----|-------------|-------------|-------------|-------------|-------------|-------------|-------|-------------|------|------|------|------|------|
| Al  | 1,00        |             |             |             |             |             |       |             |      |      |      |      |      |
| Si  | <b>0,95</b> | 1,00        |             |             |             |             |       |             |      |      |      |      |      |
| P   | 0,59        | 0,63        | 1,00        |             |             |             |       |             |      |      |      |      |      |
| K   | <b>0,88</b> | <b>0,95</b> | 0,69        | 1,00        |             |             |       |             |      |      |      |      |      |
| Ca  | 0,20        | 0,15        | 0,61        | 0,24        | 1,00        |             |       |             |      |      |      |      |      |
| Ti  | <b>0,98</b> | <b>0,97</b> | 0,62        | <b>0,89</b> | 0,22        | 1,00        |       |             |      |      |      |      |      |
| Fe  | 0,01        | -0,02       | 0,59        | 0,03        | <b>0,89</b> | 0,05        | 1,00  |             |      |      |      |      |      |
| Zn  | <b>0,86</b> | <b>0,84</b> | 0,69        | <b>0,84</b> | 0,25        | <b>0,81</b> | 0,05  | 1,00        |      |      |      |      |      |
| Br  | 0,65        | 0,51        | 0,17        | 0,46        | -0,02       | 0,61        | -0,19 | 0,46        | 1,00 |      |      |      |      |
| Sr  | 0,78        | 0,68        | 0,46        | 0,70        | 0,42        | 0,75        | 0,13  | 0,67        | 0,68 | 1,00 |      |      |      |
| Pb  | <b>0,90</b> | <b>0,96</b> | 0,69        | <b>0,95</b> | 0,17        | <b>0,90</b> | -0,01 | <b>0,91</b> | 0,44 | 0,65 | 1,00 |      |      |
| Ash | 0,80        | <b>0,80</b> | <b>0,84</b> | 0,64        | -0,22       | <b>0,80</b> | 0,65  | <b>0,83</b> | 0,54 | 0,73 | 0,35 | 1,00 |      |
| BD  | 0,26        | 0,19        | 0,59        | 0,19        | 0,62        | 0,28        | 0,67  | 0,25        | 0,15 | 0,39 | 0,19 | 0,78 | 1,00 |

**Table 4** Correlation matrix of the elements measured with XRF-CS, ash content and bulk density. There are strong correlations between Si, Al, Ti and Zr. Good correlations are also seen between the previous elements and Zn, Y and Pb. Good negative correlation between Fe and Sr exist and mostly weak to no correlation are seen throughout for P, K, Ca, Br and Sr.

|     | Al          | Si          | P     | K     | Ca    | Ti    | Fe          | Zn          | Br    | Rb    | Sr    | Y           | Zr   | Pb          | Ash  | BD   |
|-----|-------------|-------------|-------|-------|-------|-------|-------------|-------------|-------|-------|-------|-------------|------|-------------|------|------|
| Al  | 1,00        |             |       |       |       |       |             |             |       |       |       |             |      |             |      |      |
| Si  | <b>0,86</b> | 1,00        |       |       |       |       |             |             |       |       |       |             |      |             |      |      |
| P   | 0,10        | 0,14        | 1,00  |       |       |       |             |             |       |       |       |             |      |             |      |      |
| K   | 0,43        | 0,54        | 0,22  | 1,00  |       |       |             |             |       |       |       |             |      |             |      |      |
| Ca  | -0,31       | -0,48       | 0,00  | 0,06  | 1,00  |       |             |             |       |       |       |             |      |             |      |      |
| Ti  | <b>0,85</b> | <b>0,88</b> | 0,06  | 0,36  | -0,43 | 1,00  |             |             |       |       |       |             |      |             |      |      |
| Fe  | -0,36       | -0,44       | -0,20 | -0,42 | -0,21 | -0,49 | 1,00        |             |       |       |       |             |      |             |      |      |
| Zn  | <b>0,72</b> | 0,69        | 0,26  | 0,33  | -0,27 | 0,55  | -0,17       | 1,00        |       |       |       |             |      |             |      |      |
| Br  | -0,12       | -0,12       | -0,13 | 0,42  | 0,60  | -0,09 | -0,28       | -0,18       | 1,00  |       |       |             |      |             |      |      |
| Rb  | -0,11       | -0,15       | -0,27 | -0,35 | -0,46 | -0,21 | <b>0,90</b> | -0,03       | -0,41 | 1,00  |       |             |      |             |      |      |
| Sr  | 0,55        | 0,49        | 0,10  | 0,59  | 0,33  | 0,55  | -0,72       | 0,28        | 0,52  | -0,65 | 1,00  |             |      |             |      |      |
| Y   | 0,54        | 0,74        | 0,20  | 0,53  | -0,44 | 0,49  | -0,09       | <b>0,74</b> | -0,14 | 0,12  | 0,15  | 1,00        |      |             |      |      |
| Zr  | 0,71        | <b>0,91</b> | 0,09  | 0,51  | -0,51 | 0,73  | -0,22       | 0,57        | -0,12 | 0,03  | 0,32  | 0,78        | 1,00 |             |      |      |
| Pb  | 0,58        | 0,74        | 0,15  | 0,41  | -0,53 | 0,48  | 0,08        | <b>0,76</b> | -0,26 | 0,31  | 0,06  | <b>0,95</b> | 0,79 | 1,00        |      |      |
| Ash | 0,40        | 0,54        | -0,16 | 0,23  | -0,67 | 0,35  | 0,40        | 0,47        | -0,31 | 0,64  | -0,19 | <b>0,74</b> | 0,66 | <b>0,84</b> | 1,00 |      |
| BD  | 0,20        | 0,08        | 0,00  | -0,15 | -0,44 | 0,06  | 0,61        | 0,21        | -0,48 | 0,68  | -0,31 | 0,20        | 0,16 | 0,36        | 0,53 | 1,00 |

### 3.2. Ash and conservative elements

The conservative elements that were acquired through WD-XRF and XRF-CS have been plotted alongside the ash content (Fig. 4). The elemental profiles and the ash profiles display a good visual agreement as to where changes in the profiles occur. Correlations between ash and the specific profiles (Table 3. and Table 4.) suggest better agreement between the ash profile and the WD-XRF dataset compared to the XRF-CS dataset.

Assessing variation in the elemental profiles suggest there are several periods of elevated elemental concentration. To start with, all elemental profiles show increased values at the top of the profiles from around 800 cal yr BP and Al and Ti also display higher values at the bottom of the profiles below 4700 cal yr BP. In the main section of the sequence, two peaks are seen in all profiles but Y and these occur at 2400-2200 and 1500-1240 cal yr BP. Between 3700 and 2400 cal yr BP a period of fluctuating concentrations dominate. Discriminating peaks from variation in the background values have been somewhat hard, but three events can possibly be distinguished. Firstly, peaks in all elemental profiles occur at 2900 cal yr BP and is characterized by measureable Y concentrations. However, the distinct height of this peak is only represented by one sample. Secondly, two earlier periods indicate elevated elemental concentrations and these peaks contain several sample points in all profiles but Y. These periods cover 3600-3300 and 3200-3100 cal yr BP. The earliest of the two is characterized by a clear Zr peak and the later by elevated Ti levels. In total, five periods of increased concentration in conservative elements are indicated by the elemental profiles between 4700-800 cal yr BP.

The ash content varies between 0.6 and 6.4 % (Fig. 4). Maximum values are found at the top of the sequence at 420 cal yr BP and higher ash content of around 2.5 % is also seen at the bottom of the cored sequence, 5400-5000 cal yr BP. The section 5000-800 cal yr BP has an ash concentration around 1 % and three shorter periods of increased minerogenic content are seen at 4400-4200, 2400-2200 and 1240-1170 cal yr BP.

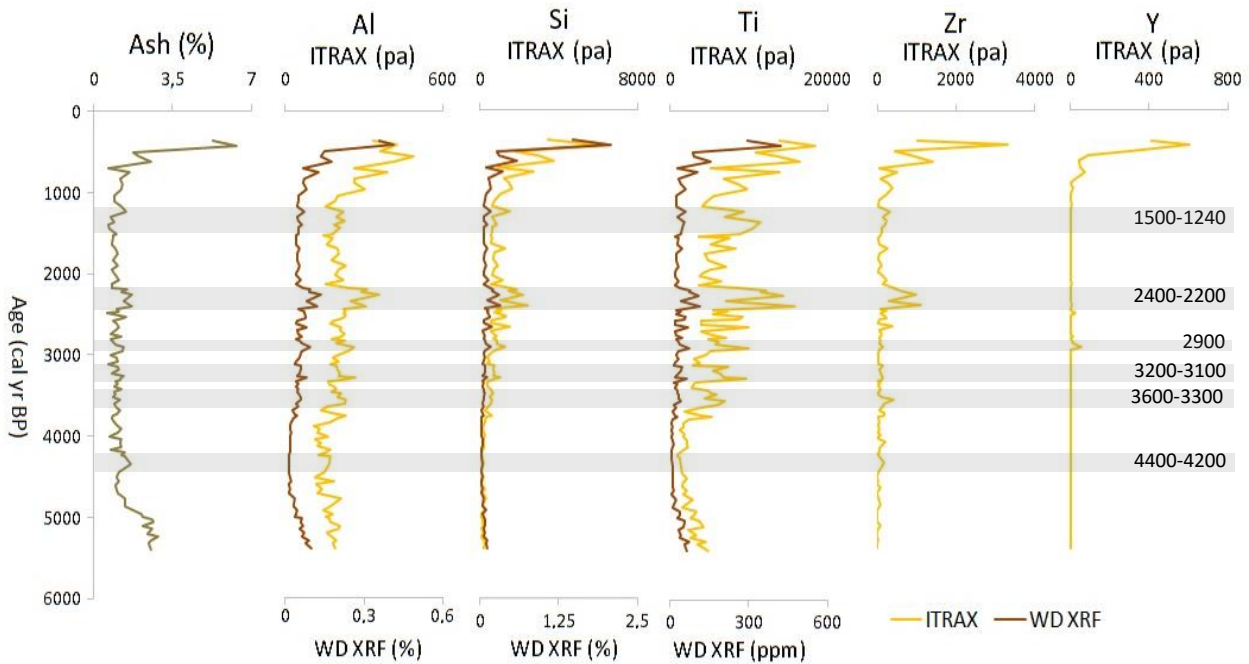


**Figure 4** Ash profile and profiles of the conservative lithogenic elements from Davidsmossen plotted with depth. Six possible dust events can be distinguished, marked in grey.

### 3.3. Organic proxies and calcium

Bulk density, C/N ratio,  $\delta^{13}\text{C}$ , peat accumulation rates and Ca are plotted in Fig. 5. Bulk density varies between 0.044 - 0.228  $\text{g}/\text{cm}^3$ , with an average of 0.091  $\text{g}/\text{cm}^3$ . Maximum values occur at 5400-4700 cal yr BP (0.100-0.228  $\text{g}/\text{cm}^3$ ), from where a clear decrease in bulk density takes place until 4300 cal yr BP (0.056  $\text{g}/\text{cm}^3$ ). 4300-3500 cal yr BP marks a period of rising bulk density (maximum at 0.134  $\text{g}/\text{cm}^3$ ) until a sharp drop to lower values (0.053  $\text{g}/\text{cm}^3$ ) occurs at 3400 cal yr BP. Lower values persist 3400-3100 cal yr BP after which a clear increase marks the onset of higher values 3100-2900 cal yr BP (0.074-0.100  $\text{g}/\text{cm}^3$ ). An overall decrease with no sharp shifts marks 2900-2400 cal yr BP. The period 2300-2100 cal yr BP begins with a sharp increase (up to 0.140  $\text{g}/\text{cm}^3$ ) and ends with a similarly sharp decrease (down to 0.060  $\text{g}/\text{cm}^3$ ). 2100-1050 cal yr BP have fluctuating bulk density between 0.040-0.096  $\text{g}/\text{cm}^3$  but with no sharp shifts. During 1050-850 cal yr BP higher bulk density values are seen again (0.100  $\text{g}/\text{cm}^3$ ), followed by lower values 800-650 cal yr BP (0.060  $\text{g}/\text{cm}^3$ ) preceding a final peak (0.170  $\text{g}/\text{cm}^3$ ) 550-400 cal yr BP after which the values decline to the top of the profile with bulk density of 0.090  $\text{g}/\text{cm}^3$  at 350 cal yr BP.

C/N ratio ranges between 27-114, with an average of 70. Starting at low values (35 at 5400 cal yr BP) the ratio increases slowly to ca 4700 cal yr BP, then more sharply rises to 4300 cal yr BP (106). Three periods of higher C/N ratios can be seen after 4700 cal yr BP: at 4300-3650 cal yr BP (80-106), 2700-2300 cal yr BP (62-111) and 1600-1300 cal yr BP (89-113). Subsequently, two periods of lower C/N ratios are recorded at 3600-2700 cal yr BP (56-73) and 2250-1700 cal yr BP (55-88). The C/N values decrease from 86 at 1300 cal yr BP and to 27 at the top of the profile.

Peat accumulation changes greatly along the length of the sequence, ranging from 34 to 216  $\text{g}/\text{m}^2/\text{yr}$ . Maximum values are seen around 5000 cal yr BP (216  $\text{g}/\text{m}^2/\text{yr}$ ), from where a decline occurs to 94  $\text{g}/\text{m}^2/\text{yr}$  at 4700 cal yr BP. A continuing decline to 67  $\text{g}/\text{m}^2/\text{yr}$  at 4300 cal yr BP is followed by a steady increase to 3500 cal yr BP (157  $\text{g}/\text{m}^2/\text{yr}$ ) where a drop to lower values (65  $\text{g}/\text{m}^2/\text{yr}$ ) occurs and persist to 3100 cal yr BP. A period of higher rates 3000-2500 cal yr BP (84-104  $\text{g}/\text{m}^2/\text{yr}$ ) is followed by a short

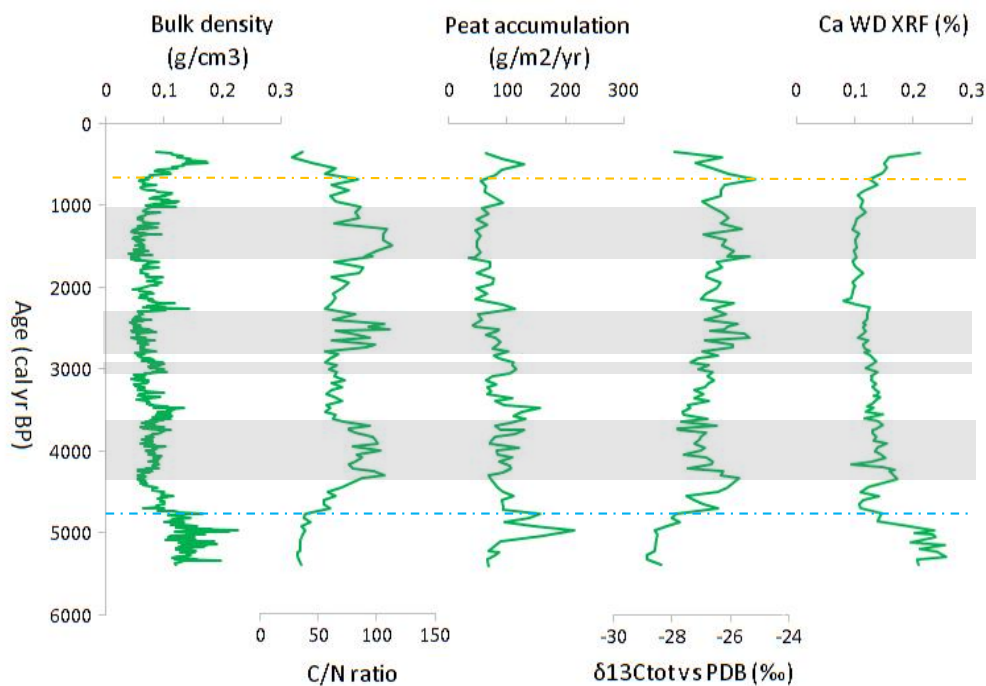


**Figure 5** Bulk density, C/N ratio,  $\delta^{13}\text{C}$ , peat accumulation and calcium from WD-XRF are plotted with depth to display the proxies related to bog development. The fen-bog transition occurs at 4700 cal yr BP (blue, dotted line) and the acrotelm-catotelm boundary, or possible deepest effect of drainage, begin around 800 cal yr BP (yellow, dotted line).

period of lower values (40 g/m<sup>2</sup>/yr) 2450-2300 cal yr BP adjacent to a distinct peak (112 g/m<sup>2</sup>/yr) at 2250 cal yr BP. The period 2100-700 cal yr BP have peat accumulation ranging from 34-92 g/m<sup>2</sup>/yr and is preceding a final peak of 129 g/m<sup>2</sup>/yr at 500 cal yr BP before the top of the profile (64 g/m<sup>2</sup>/yr). The average peat growth at Davidsmossen is 0.98 mm/yr, average peat accumulation is 86 g/m<sup>2</sup>/yr and average carbon accumulation is 42 g/m<sup>2</sup>/yr (carbon accumulation is not shown).

$\delta^{13}\text{C}$  ranges from -29 to -25 ‰. A steady increase is seen from the base of the profile (-28.8 ‰) up to ca 4700 cal yr BP, from which point the values stay above -28 ‰. The increase then continues up to 4300 cal yr BP and reaches a  $\delta^{13}\text{C}$  value of -25.7 ‰. A slight decrease down to -27.8 ‰ at 3700 cal yr BP is followed by a small increase to 3300 cal yr BP (-26.8 ‰), a decrease to -27.4 at 2900 cal yr BP and then an increase to -25.5 ‰ at 2600 cal yr BP. After this point the  $\delta^{13}\text{C}$  value fluctuates between -27 and -25 ‰ up to 700 cal yr BP from where a clear decrease lowers the  $\delta^{13}\text{C}$  value to -27.9 ‰ at the top of the profile.

Total carbon (TC) (not shown) varies between 43.8 and 58.0 % through the peat sequence and the average TC is 48.6 %. Total nitrogen (TN) (not shown) varies between 0.5 and 2.0 % through the peat sequence and the average TN is 0.9%.

The calcium profile from WD-XRF (Fig. 5) displays high values (0.20-0.26 %) from the bottom of the profile to 5000 cal yr BP, from where a steep decline occurs to 0.11 % at 4700 cal yr BP. Increasing Ca-values are seen 4700-4300 cal yr BP where the Ca reaches 0.17 %. From here an overall decrease to 1300 cal yr BP (0.10 %) can be seen with two marked drops occurring at 4150 cal yr BP (0.09 %) and at 2170 cal yr BP (0.08 %). At 1300 cal yr BP the profile trend shifts and increasing Ca-amounts can be seen to the top of the profile (0.21 %).

In summary, all profiles indicate change at 4700 cal yr BP. The clearest changes are seen in the C/N data which display three periods of relatively higher values and three of lower values. A change in the C/N ratio from high to low values are accompanied by a rise in bulk density and higher peat accumulation, but a few bulk density shifts are seen at other times as well.

## 4. Discussion

### 4.1. Comparison of WD-XRF and XRF-CS

WD-XRF and XRF-CS have the same basic analytical principle of exciting atoms and both methods perform non-destructive multi-elemental analysis. However, there are several differences as well. To start with the XRF-CS gives relative measurements and it has the ability to perform measurements continuously along the surface of a core (down to 200  $\mu\text{m}$  resolution), though it was used on separate samples in this project. Comparably, WD-XRF gives absolute values but due to processing can generate negative values, as seen here for Rb. Producing absolute values has the advantage of allowing assessment of the results in regard to accuracy and precision and comparison with other sites and standards. In this project the two methods were used on samples with different sample preparation steps: milled bulk peat and ashed peats, in order to evaluate if the XRF-CS results can be used for geochemical analysis of dust related elements in peat.

Generally, good agreement in the shape of the elemental profiles between the two XRF methods could be seen. Though, the profiles from the XRF-CS appears to vary more than the profiles from WD-XRF. The bivariate correlations confirmed strong correlation between the results from the two methods for Pb, Fe, Zn and Si ( $r = 0.84-0.91$ ) and fairly strong correlation for Al, K and Ti ( $r = 0.66-0.73$ ). These elements have been shown to not be affected or only show small decreases during dry ashing at 450°C (Koh, *et al.*, 1999). Of the elements with no to very low correlation (Sr, Ca, P, Rb and Br) Br is the only element that has been shown to be volatile at 450°C (Koh *et al.* 1999). Loss of Br could therefore be a plausible explanation for the change in its profile shape between the methods. The weak correlation for Rb is explained for by the WD-XRF methods inability to measure the low Rb-concentrations in the peat

sample. However, the general differences in the elemental profiles and the changed curvature of Sr, P and especially Ca are harder to explain and are probably caused by multiple factors.

Visually the two profiles for Sr, P and Ca from WD-XRF and XRF-CS are not so different. A generally higher internal variation in the XRF-CS dataset could perhaps explain some of the differences. Previous studies have shown good correlations between WD-XRF and XRF-CS results, but also there a greater variation in the XRF-CS data was observed. This pattern of captured but amplified variation in XRF-CS data compared to WD-XRF data has been presented by Croudace *et al.* (Fig. 4, 2006). More variation in XRF-CS data compared to collision reaction cell inductively coupled plasma quadrupole mass spectrometry (CRC-ICP-MS) was shown by Poto *et al.* (2015) who compared results of major and trace elements. Their findings showed that there were perfect to high correlation between the methods for several elements and moderate correlations for others, even though their elemental profiles showed variation similar to the profiles presented here.

However, in these two studies a possible explanation for the variation in the XRF-CS result comes from the different resolution of the two methods, where the CRC-ICP-MS and WD-XRF have been performed at 1 cm resolution and 200-250  $\mu\text{m}$ , respectively. The XRF-CS data could show actual variations the two other methods missed. Another explanation would be that the XRF-CS data is more variable in nature. The latter explanation would also account for some of the variation seen in the XRF-CS data presented here compared to that of the WD-XRF.

Differences in the results for the two methods could also be related to the different types of samples used. The WD-XRF analysis was performed on milled bulk peat containing up to 99 % organic matter. This can perhaps weaken the elemental signal from the minerogenic fraction as described for organic matrices by Croudace *et al.* (2006). Furthermore, the sample material was heterogeneous (e.g. *Sphagnum* and *Carex*) which could affect the result through matrix related effects. However, milling should have reduced the risk of such interferences. The samples measured with WD-XRF weighed in between 420-525 mg, not far from the range of 500mg  $\pm$ 50 mg suggested for optimal analytical performance. A few samples were a little too small and weighed in under 450mg. As shown by Rydberg (2014), who performed analyses on loose powder sediments, deviations in sample weight can have effects on the elemental concentrations for elements heavier than As.

The XRF-CS analyses were performed directly on the minerogenic fraction (assumed to equal the ash content) and the elemental signals could be amplified in the absence of “diluting” organic matter. Enhancement of the minerogenic signal could perhaps result in some of the greater variation seen for XRF-CS data. Though, a downside of analysing ash is that the sample size becomes very small since the dust content is so low. Not all cups could be fully filled and this generated compaction and porosity differences in the samples, which have been shown to effect the result of XRF-CS (Croudace *et al.*, 2006). Deviating values could be seen for at least one sample that was particularly small and only had a half-full sample cup, which thus resulted in poor analytical quality.

Considering that there are a number of possible explanations for the changed shape of elemental profiles retrieved for the two XRF methods, determining which one/ones caused the changes is difficult. Despite all the possible interferences of the two XRF methods, the results showed generally good agreement. Especially the conservative elements, of interest in determining dust deposition, kept their profile curvature in both analyses and implied relative changes at the same time in both datasets. As the accuracy and precision was good for the WD-XRF measurements and the XRF-CS data showed the same relative changes, it can be concluded that XRF-CS on ashed peats is an alternative to the more conventional WD-XRF technique.

## 4.2. Organic proxies and peatland development

### 4.2.1. Organic proxies at Davidsmosse

The average bulk density, carbon and nitrogen content and C/N ratio observed in the peat sequence are typical of northern peatlands (Loisel *et al.*, 2014). However, the carbon accumulation rate is higher at Davidsmosse than the average presented by Loisel *et al.* (2014) and the average peat growth (0.98mm/yr) is higher than the average peat growth at nearby Store Mosse (0.79 mm/yr, Kylander *et al.* 2013). Higher peat accumulation and subsequent carbon accumulation are not surprising results as Davidsmosse have 5 m peat accumulation corresponding to 5400 yr, compared to other Swedish bogs such as Store Mosse where 5.5 m peat equals 8900 years (Kylander *et al.*, review) and Stömyren (380 km to the north, Värmland) where 1.9 m equals 8000 yr of peat accumulation (Gunnarson *et al.*, 2001). The growth rate has clearly been higher at Davidsmosse which makes this bog of particular interest in paleoclimate studies because it provides an archive of higher resolution.

### 4.2.2. Fen-bog transition

In Davidsmosse several changes are seen occurring simultaneously at 4700 cal yr BP (see Fig. 3, 4 and 5). Decreases in the redox sensitive elements (Ca and Fe), the minerogenic content and bulk density co-occur with increasing C/N ratio. These concurrent changes have been interpreted to mark the fen-bog transition. Firstly, a transition from fen to bog is characterized by a drop in bulk density and a corresponding increase in C/N ratio. This shift represents the transition from non-*Sphagnum* species in the fen (higher bulk density, lower C/N ratio) to mostly *Sphagnum* species in the bog (lower bulk density, higher C/N ratio) (Kuhry and Vitt, 1996; Loisel *et al.*, 2014).

Secondly, a clear increase is also seen in  $\delta^{13}\text{C}$  between 5400 and 4700 cal yr BP. The  $\delta^{13}\text{C}$ -value in *Sphagnum* is affected by several factors including temperature, altitude, *Sphagnum* type (Ménot and Burns, 2001) and wetness (Chambers *et al.*, 2012 and sources therein). All  $\delta^{13}\text{C}$ -values seen at Davidsmosse are typical of C3 plants (O'Leary, 1988) but the changes could still be indicative of a shift in dominating plant species or climate/wetness. Ménot and Burns (2001) concludes that when there are only C3 plants in a peat sequence, changes in the  $\delta^{13}\text{C}$  have to be interpreted in regard to changes in species and cannot be inferred as an individual proxy of climate conditions. Nevertheless, in this case interpreting the increase in  $\delta^{13}\text{C}$ -values as a shift in plants species, changed wetness or a combination of both would all be explanations that agrees with this shift occurring across the fen-bog transition.

Together these changes suggest the transition from a fen with minerotrophic conditions (flowing water contributing with minerals and nutrients) to a bog with ombrotrophic condition (receiving all its input from the atmosphere). This is also supported by the ash-profile in which the content decreases at 4700 cal yr BP and remains low throughout the main section of the peat sequence to about 800 cal yr BP when the amount of ash increases again. The low ash amounts reflect dust deposition typical of ombrotrophic bogs (Tolonen, 1984). As such, the peat sequence older than 4700 cal yr BP is not optimal for reconstruction of changes in atmospheric dust deposition since the input of mineral matter through water flow will likely overprint the atmospheric dust signal. The presence of flowing water also makes interpretations of the elemental signals more uncertain since it is possible elements have moved in relation to where they were deposited. As for mobile elements, diffusion from the underlying fen to the ombrotrophic bog can be seen as higher values at the bottom of the profiles for Fe and Ca.

### 4.2.3. Humidity changes

Peat as a record of humidity, in terms of wetter and drier conditions, assumes that more decomposed layers have developed during drier periods and less decomposed layers have formed during wetter periods. A lowered water table would expose more of the organic matter to oxic conditions and more decay can take place. By contrast, wetter periods keep the water table high and less decomposition occurs as the anoxic conditions of the catotelm reaches higher and slows decomposition. Hansson *et al.* (2013) studied three types of proxies generally used for determining decomposition in peat. Their results

showed that bulk density, C/N ratio and light transmission show different aspects of the decay process in a peat bog and they suggest that more than one proxy is used as decomposition is not completely explained by one single proxies.

Here, bulk density and C/N ratio have been used as proxies for decomposition. Bulk density can be assumed to be higher in more decomposed layers as the organic matrix is weakened and compacted as more peat accumulates on top (Johnson *et al.*, 1990). However, bulk density is also affected by plant species (Loisel *et al.*, 2014). Decomposition has been linked to changes in C/N ratio due to preferential loss of carbon during decomposition (Kuhry and Vitt, 1996). Lower C/N ratios can thus be indicative of more decomposed peat as a result of relative nitrogen enrichment, and higher C/N ratio reflect more of the relationship between carbon and nitrogen in fresh *Sphagnum*. However, the C/N ratio is also controlled by plant type as shown by the data compiled by Loisel *et al.* (2014). In Davidsmosse, where *Sphagnum* ssp. dominate the main part of the sequence, C/N ratio can be assumed to mainly be controlled by decay processes. Thus, low C/N ratio indicate drier conditions and high C/N ratio wetter periods.

Judging by the C/N ratio, there have been three periods of wetter condition: 4300-3650, 2740-2300 and 1600-1300 cal yr BP. And two periods of prevailing dry condition: 3600-2700 and 2250-1700 cal yr BP. These transitions agree well with bulk density changes which can indicate shifts from wetter to drier conditions, as decomposition can be assumed to increase in such periods of change, when the water table might be lowered. Higher bulk density can be seen 3500-3400 and 2300-2100 cal yr BP, corresponding to C/N indicated humidity shifts from wet to dry. Another bulk density peak at 1050-800 cal yr BP match to the onset of declining C/N values (drier conditions) to the top of the profile, and the topmost peak in bulk density could be indicative of the periodically drier conditions of the acrotelm or the result of drainage. One more period of increased bulk density was identified 3100-2900 cal yr BP. This period does not have a corresponding wet-dry shift indicated by the C/N ratio, but could nonetheless be indicative of a humidity shift. It could also result from a shift in dominating plant species, which possibly is supported by a drop in  $\delta^{13}\text{C}$ , but that would have to be confirmed with macrofossils.

### 4.3. Elemental variations and dust event

#### 4.3.1. Elemental variation

Results from the ashing showed that the minerogenic content of Davidsmosse was low, typical of ombrotrophic peat bogs (Tolonen, 1984). Yet, apart from Rb the elements analysed here were present in measurable quantities with both XRF methods. Of the 14 elements analysed several different elemental behaviours can be discerned. Firstly, Pb and Zn have shown very strong correlation ( $r = 0.91$ ) and distinguish themselves from the other elements by being present in high concentration in the top of the sequence and then being just above detection limit at a few older locations. Pb has been linked to mining, and later to lead gasoline and industries releasing anthropogenic pollution. High Pb values are seen at the top of the profile ( $> 1000$  cal yr BP), after which Pb appears just above the detection limit at a period covering a few hundred years around 2000 cal yr BP, which is equivalent to the Roman empire, and around 4000 cal yr BP. Lead pollution has previously been analysed in ombrotrophic bogs in Sweden (e.g. Dumme Mosse, Århultsmyren, Store Mosse) and changes seen in these records are time synchronous to those at Davidsmosse (Klaminder *et al.*, 2013; Kylander *et al.*, 2013). Anthropogenic influences have thus occurred at several occasions during the bog development. Zn follows Pb very closely and though it has been discussed whether it behaves mobile or not in peat deposits (De Vleeschouwer *et al.*, 2009), it appears to behave like a conservative pollutant at Davidsmosse.

Secondly, the redox sensitive Fe and Ca displays similar behaviour, which is supported by a strong correlation ( $r = 0.89$ ). They are clearly present in the lowermost fen-layer influenced by flowing water and only exists in smaller concentration in the ombrotrophic part of the profile, indicating they behave mobile in Davidsmosse.

Thirdly, we have the elements that are lithogenic elements, but have other capacities as well. Among these we find P, K, Sr, Rb and Ca. However, here these display varying behaviour indicating they are at least controlled by one other variable than mineralogical input.

This leaves Al, Si, Ti, Zr and Y which display strong similarities in their profiles and also show high correlations ( $r = 0.71-0.91$  (Al-Y,  $r = 0.54$ ) for XRF-CS;  $r = 0.95-0.98$  for WD-XRF). The elemental concentrations retrieved by WD-XRF for these elements also correlate well with the ash content ( $r = 0.8$ ) and elemental profiles from both methods display good similarity with the ash profile (Fig. 4), indicating they are indeed the conservative lithogenic elements in Davidsmosse.

#### 4.3.2. Dust events

Based on the variation in the conservative lithogenic elements, it appears that several dust events have occurred during the last 5400 years. Three events have been found close together, separated by only a few centuries. The first event occurred at around 3600-3300 cal yr BP and is characterised by a clear peak in Zr. The second rise in conservative elements interpreted as a dust peak follows at 3200-3100 cal yr BP and has a distinct rise in Ti. The third peak is the most uncertain but is distinguished through measurable Y amounts, at 2900 cal yr BP. A fourth peak is clearly seen in the elemental profiles of Al, Si, Ti and Zr, and this is also the first peak where a corresponding increase can be seen in the ash profile. The latest dust event identified occurred 1500-1240 cal yr BP and is also seen in both the elemental profiles and in the ash profile. After 1000 cal yr BP the ash content and the elemental profiles all show steep increase. This is probably not related to natural dust deposition but has other causes such as biological enrichment, increased human activities causing increased deposition and/or desiccation of the peat due to drainage.

Determining the dust events solely from the ash profile would indicate that there only have been two events, and the duration of the second event would be shortened and delayed to 1240-1170 cal yr BP. A third possible peak is seen 4440-4250 cal yr BP, but this peak occurs close to the fen-bog transition (section 4.3.1.) and is therefore hard to interpret with certainty. It is followed by a possible rise in Al but no increases are seen in the other elemental profiles.

When discussing dust in ombrotrophic bogs peat accumulation and decomposition have to be mentioned. All peaks seen are not necessarily dust events as enrichment of mineralogical material can happen if, for example, peat accumulation have been slow as suggested by Weiss *et al.* (2001). This is the case for the possible event at 4440-4250 cal yr BP, it coincides with a drop in peat accumulation indicating this peak might be an enrichment of conservative elements of other origin than increased dust deposition. For the other five peaks peat accumulation have been slightly higher to much higher than for surrounding time periods so enrichment due to slowed peat accumulation is not likely. Decomposition based on bulk density suggest that the peaks 4440-4250, 3200-3100, 2900 and 1500-1200 (-1100) cal yr BP are not influenced by high decomposition either. However, the peaks at 3600-3400 and 2400-2200 are accompanied by higher bulk density and could thus be artefacts in the record. Especially the older peak, who lacks a corresponding ash peak. High decomposition could explain some of the extra peak height seen at 2400-2200 cal yr BP in several of the profiles.

### 4.4. Changes in dust deposition and effective humidity

#### 4.4.1. The record of Davidsmosse

Compiling the results from Davidsmosse shows that there have been six possible dust events during the last 5400 years and several changes in effective humidity (Fig. 6). The first dust event (1) (4400-4200 cal yr BP) precedes and overlaps with the first period of wetter conditions (4300-3650 cal yr BP) as indicated by the C/N ratio. A sharp shift to drier conditions (3650-3600 cal yr BP) mark the onset of the second dust event (2), 3600-3300 cal yr BP. Higher bulk density is also seen at this time, which supports the idea that the climate has shifted from wet to dry, causing a lowering of the water table and increased decomposition. This dry period persists to 2700 cal yr BP, covering both dust event 3 and 4 (3200-3100

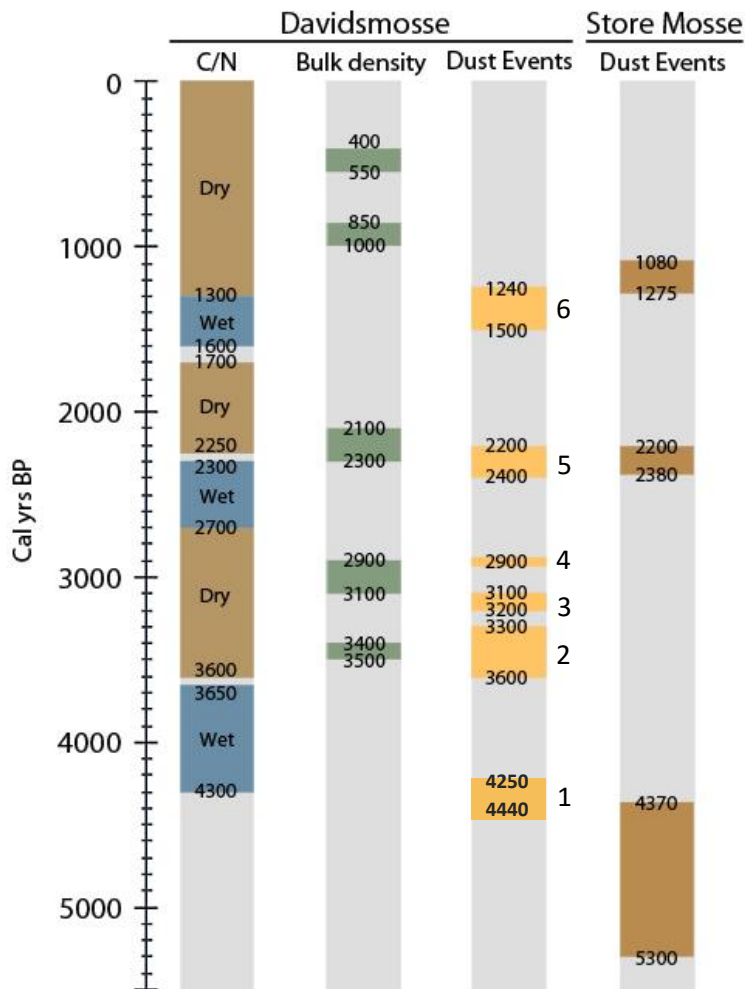


**Figure 6** Compilation of the possible dust events, the most distinct bulk density shifts and variation in C/N ratio from Davidsmossen compared with the dust events established at Store Mosse by Kylander et al. (2013; in review). A generally good agreement is seen between humidity shifts (wet/dry) and dust events and a very good agreement is seen between the two latest dust events in the two bogs.

and 2900 cal yr BP). A very good agreement between dust events and drier condition is suggested from this time period. However, one bulk density peak is seen in the second half of the dry period (3100-2900 cal yr BP) that do not seem to have a corresponding shift in C/N ratio. As discussed before this peak could have several explanations, but when comparing it to the dust events, this bulk density peak fits in exactly between dust event 3 and 4. The lack of dust could indicate that this was a wetter period, though that cannot be derived from the decomposition proxies. A second explanation would be if the bog entered a new stage and a change in dominating *Sphagnum* ssp. occurred. Several bog stages have been identified in Store Mosse (Svensson, 1988; Kylander, 2013) and it is likely that there have been multiple stages at Davidsmossen as well. However, that is speculation and would have to be confirmed by identification of the *Sphagnum* species in the peat stratigraphy.

During the following wet period (2700-2300 cal yr BP) the other proxies are relatively stable, until the end when dust event 5 (2400-2200 cal yr BP) begins. It is shortly after followed by increased bulk density, as expected when shifting from wetter to dryer conditions. The dry period continues for several hundred years after dust event 5, without any new dust events being recognised.

Halfway through the last period of wetter conditions (1600-1300 cal yr BP) the rise in conservative elements begins, indicating the start of dust event 6 which then stretches into the following and final dry period. If defining dust event 6 from the ash profile (1240-1170 cal yr BP) the entire event takes place

during the period of dry conditions. Two bulk density increases take place after the last C/N indicated humidity shift, and the earlier (1000-850 cal yr BP) can probably indicate the last major transition from wet to dry conditions. It could also be an event unrelated to naturally changing conditions from wet to dry and instead be caused by anthropogenic doings, such as drainage. The topmost bulk density increase is definitely close to the acrotelm-catotelm boundary, if not indicating its exact position. In summary, the proxies compiled from Davidsmosse show that dust deposition have since mid-Holocene and six possible dust events have been recognised. A pattern of concurrent changes between indicators of humidity and of paleodust arises, where a period of wetter condition is followed by a dust event and a transition to drier conditions, indicated by both C/N ratio and bulk density.

#### 4.4.2. Dust records from Davidsmosse and Store Mosse

One of the goals for this project was to compose a dust record for comparison with the findings at nearby Store Mosse. In Fig. 6 the dust events reported by Kylander (2013; in review) are shown together with the results from Davidsmosse. Of the four dust events identified in Store Mosse, three occur in the period covered by Davidsmosse. The oldest Store Mosse event, 5300-4370 cal yr BP, correspond with the fen stage at Davidsmosse, and the transition into ombrotrophic conditions. Thus, a fully matching dust event does not exist. However, dust event 1, 4440-4250 cal yr BP, which is the most uncertain one due to its closeness to the fen-bog transition, do display overlap with the dust event reported from Store Mosse, indicating it is a proper dust event.

During the following 2000 years no dust events are found at Store Mosse, so no co-occurring events are seen for dust event 2, 3 and 4. Dust event 5 (2400-2200 cal yr BP), on the contrary, show superb agreement with a corresponding dust event in Store Mosse occurring 2380-2200 cal yr BP. Equally good agreement is seen for the dust event in Store Mosse dated to 1275-1080 cal yr BP compared with dust event 6 (1500-1240 cal yr BP), especially if defining the extension of dust event 6 from the ash profile (1240-1170 cal yr BP) instead of the elemental profile.

A local origin of close to Davidsmosse could explain why no matching events were found for dust event 2, 3 and 4. The differences could also be due to the two different methods applied to inferring changes in the dust record. Here, dust events were identified by visually assessing the profiles and comparing correlations. In Store Mosse principle component analysis and change point modelling was used to statistically identify changes in the dust deposition record (Kylander *et al.*, 2013). Conclusively, very good agreement was found between three of the possible dust events found in Davidsmosse to the three previously identified dust events in Store Mosse. This agreement between two bogs 60 km apart suggest the dust events were of regional scale.

#### 4.4.3. A second humidity record from peat and dendrochronology

A record of humidity compiled from dendrochronology and peat stratigraphy in Sweden, reported by Gunnarson *et al.*, (2003), have also identified several periods of alternatingly drier and wetter conditions. The peat stratigraphy was performed on a sequence from Stömyren, Värmland, about 380 km north of Davidsmosse. Several of the identified periods coincide well with the periods of elevated dust deposition found at Davidsmosse. Dust event 1 at 4440-4250 cal yr BP correlates precisely to a dry period identified at 4400-4200 yr BP by Gunnarson *et al.* (2003). Dust event 2, 3600-3300 cal yr BP, occurs at a transition from wet (3700-3500 yr BP) to dry conditions (3500-3100 yr BP). This dry period also persists over dust event 3 (3200-3100 cal yr BP), ending synchronously. The short dust event 4, at 2900 cal yr BP, coincides with the end of a wet period identified 3100-2900 yr BP. This wet period is interesting, since it spans just across that period of elevated bulk density discussed in section 4.4.1., regarding whether it could represent a wet period or not. Comparing to this record, the increased bulk density at 3100-2900 cal yr in Davidsmosse can be interpreted as a wet event.

The pronounced dust event 5 (2400-2200 cal yr BP) does not correlate to a specific humidity as there is a gap 2900 to 2100 cal yr BP in the record compiled by Gunnarson *et al.* (2003). However, dust event 5 precedes an interpreted wet event 2100-1950 yr BP indicating the dust event occurred in relatively dry

conditions. Finally, the onset of the last dust event (1500-1240 cal yr BP) coincides with a period of dry conditions (1600-1400 yr BP) and ends with the beginning of a new wet period (1250-1100 yr BP). The dust events show good agreement with the humidity fluctuations presented by Gunnarson *et al.* (2003), which supports the idea that these are naturally occurring, climate induced events.

## 5. Conclusion

The aim of this project was to reconstruct changes in paleoenvironmental conditions in southwest Sweden over the last 5400 cal yr BP in regard to dust deposition and general trends in humidity. The specific objectives were to (i) compare the results from WD-XRF on bulk peat and XRF-CS on ashed peats and (ii) reconstruct changes in mineral dust deposition and effective humidity.

The results from the two XRF-methods showed generally good correlation between the elemental variations acquired and the strongest correlations were found for the conservative lithogenic elements and the pollutants. WD-XRF on milled bulk peat and XRF-CS on ashed peats, deal with separate sample matrix related issues. However, the results were good for WD-XRF and the method using a XRF-CS to analyse ashed peat samples displayed the same relative changes for most elements. As far as it can be concluded from the limited set of samples analysed here, that XRF-CS on ashed peat is an applicable alternative to the more conventional WD-XRF technique when relative changes are wanted.

A multi-proxy approach was used to determine past dust deposition and humidity changes at Davidsmosse. Bulk density, C/N ratio,  $\delta^{13}\text{C}$ , peat accumulation, ash content and a set of 14 elements were used here. Six possible periods of elevated dust deposition since mid-Holocene have been identified: 4440-4250, 3600-3300, 3250-3100, 2900, 2400-2200 and 1500-1200 cal yr BP. The earliest and the two latest dust events agree very well in time with events found in the dust record compiled by Kylander *et al.* (2013) from Store Mosse. Agreement in time between these period of elevated dust found in two ombrotrophic bogs located 60 km apart, suggest that the dust events were of regional scale. Additionally, three periods of predominantly wetter conditions (4300-3650, 2700-2300 and 1600-1300 cal yr BP) and three periods of drier conditions (3600-2700, 2250-1700 and 1300-present cal yr BP) were interpreted from the multi proxy record retrieved from Davidsmosse. The humidity shifts occur in good agreement with the dust events suggesting a close link between effective humidity and atmospheric mineral dust.

## Acknowledgements

First and foremost, my supervisor Malin Kylander is thanked for her indispensable guidance and encouragement. Johan Rydberg and Richard Bindler are thanked for their instructions and help with the WD-XRF at the Department of Ecology and Environmental Science, Umeå University. Acknowledgement go to Jenny Sjögren for introducing the Clam program - keep Clam and carry on.

## References

- Blaauw, M. (2010): Methods and code for “classical” age-modelling of radiocarbon sequences. *Quaternary Geochronology*. 5. pp 512-518
- Blytt, A.G. (1876): Essay on the Immigration of the Norwegian Flora during Alternating Rainy and Dry Periods. Cammermayer, Kristiana.
- Blytt, A.G. (1882): Die theorie der wechselnden kontinentalen und insularen klimare. *Botanische Jahrbücher für Systematik. Pflanzengeschichte und Pflanzengeographie*. 2. pp. 1-50

- Chambers, F., Booth, R., De Vleeschouwer, F., Lamentowicz, Le Roux, G., Mauquoy, D., Nichols, J. & van Geel, B. (2012): Development and refinement of proxy-climate indicators from peat. *Quaternary International*. 268. pp. 21-33
- Croudace, I. W., Rindby, A. & Rothwell, R. G. (2006): ITRAX: description and evaluation of a new multi-function X-ray core scanner. In: Rothwell, R. G. (Ed.): *New techniques in sediment core analysis*. Geological Society. London. Special Publications. 267. pp. 51-63.
- De Jong, R., Björck, S., Björkman, L. & Clemmensen, L. (2006): Storminess variation during the last 6500 years as recorded from an ombrotrophic peat bog in Halland, southwest Sweden. *Journal of Quaternary science*. 21. 8. pp. 905-919
- De la Rosa, G., Peralta-Videa, JR. & Gardea-Torresdey, JL. (2003): Utilization of ICP/OES for the determination of trace metal binding to different humic fractions. *Journal of Hazardous materials*. B97. pp. 207-218.
- De Vleeschouwer, F., fagel, N., Cheburkin, A., Pazdur, A., Sikorski, J., Mattielli, N., Renson, V., Fialkiewicz, B., Piotrowska, N., Le Roux, G. (2009): Anthropogenic impacts in North Poland over the last 1300 years – A record of Pb, Zn, Cu, Ni and S in an ombrotrophic peat bog. *Science of the Total Environment*. 407. pp. 5674-5684
- Gunnarson, B., Borgmark, A. & Wastegård, S. (2003): Holocene humidity fluctuations in Sweden inferred from dendrochronology and peat stratigraphy. *Boreas*. 32. 2. pp. 347-360
- Hansson, S., Rydberg, J., Kylander, M., Gallagher, K. & Bindler, R. (2013): Evaluating paleoproxies for peat decomposition and their relationship to peat geochemistry. *The Holocene*. 23. pp. 1666-1671
- Johnson, L., Damman, A. & Malmer, N. (1990): Sphagnum macrostructure as an indicator of decay and compaction in peat cores from ombrotrophic south Swedish peat-bog. *Journal of ecology*. 78. pp. 633-647
- Khury, P. & Vitt, D. H. (1996): Fossil Carbon/Nitrogen ratios as a measurement of peat decomposition. *Ecology*. 77 (1). pp. 271-275
- Klaminder, J., Renberg, I., Bindler, R. & Emteryd, O. (2003): Isotopic trends and background fluxes of atmospheric lead in northern Europe: Analyses of three ombrotrophic bogs from south Sweden. *Global biogeochemical cycles*. 17.
- Koh, S., Aoki, T., Katayama, Y. and Takada, J. (1999): Losses of elements in plant samples under the dry ashing process. *Journal of the radioanalytical and nuclear chemistry*. 229. 3. pp. 591-594
- Kohfeld, K. E. & Harrison, S. (2001): DIRTMAP: the geological record of dust. *Earth-Science Reviews*. 54. pp. 81–114.
- Kylander, M., Bindler, R., Martínez Coritaz, A., Gallagher, K., Mörth, C.-M. & Rauch, S. (2013): A novel geochemical approach to paleorecords of dust deposition and effective humidity: 8500 years of peat accumulation at Store Mosse (the “Great Bog”). Sweden. *Quaternary Science Reviews*. 69. pp. 69-82
- Kylander, M., Martínez-Cortizas, A., Bindler, R., Greenwood, S., Mörth, M. & Rauch, S. (in review, jan 2016): Characterizing changes in mineral dust during the Holocene in southern Sweden: The Store Mosse (the “Great Bog”) record. Submitted to *Geochimica et Cosmochimica Acta*.
- Loisel, J., Yu, Z., Beilman, D., Camill, P., Alm, J., Amesbury, M., Anderson, D., Andersson, S., Bochicchio, C., Barber, K., Belyea, L., Bunbury, J., Chambers, F., Charman, D., De Vleeschouwer, F., Fialkiewicz-Kozielec, B., Finkelstein, S., Gałka, M., Garneau, M., Hammarlund, D., Hinchcliffe,

- W., Holmquist, J., Hughes, P., Jones, M., Klein, E., Kokfelt, U., Korhola, A., Kuhry, P., Lamarre, A., Lamentowicz, M., Large, D., Lavoie, M., MacDonald, G., Magnan, G., Mäkilä, M., Mallon, G., Mathijssen, P., Mauquoy, D., McCarroll, J., Moore, T., Nichols, J., O'Reilly, B., Oksanen, P., Packalen, M., Peteet, D., Richard, P., Robinson, S., Ronkainen, T., Rundgren, M., Sannel, B., Tarnocai, C., Thom, T., Tuittila, E., Turetsky, M., Väliranta, M., van der Linden, M., van Geel, B., van Bellen, S., Vitt, D., Zhao, Y. & Zhou, W. (2014): A database and synthesis of northern peatland soil properties and Holocene carbon and nitrogen accumulation. *The Holocene*. 24. pp. 1028-1042
- Margalef, O., Martínez-Cortizas, A., Kylander, M., Pla-Rabes, S., Cañellas-Bolta, N., Pueyo, J.J., Sáez, A., Valero-Garcés, B.L. & Giralt, S. (2014): Environmental processes in Rano Aroi (Easter Island) peat geochemistry forced by climate variability during the last 70 kyr. *Paleogeography, Paleoclimatology, Paleoecology*. 414. pp. 438-450
- Martínez Cortizas, A., Peiteado Varela, E., Bindler, R., Biester, H. & Cheburkin, A. (2012): Reconstructing historical Pb and Hg pollution in NW Spain using multiple cores from Chao de Lamoso bog (Xistral Mountains). *Geochim Cosmochim Acta*. 82. pp. 68–78
- Ménot, G. & Burns, S. (2001): Carbon isotopes in ombrogenic peat bog plants as climatic indicators: calibration from an altitudinal transect in Switzerland. *Organic Geochemistry*. 32. pp. 233-245
- Muller, J., Kylander, M., Martínez-Cortizas, A., Wüst, R., Weiss, D., Blake, K., Coles, B. & Garcia-Sanchez, R. (2007): The use of principle component analyses in characterising trace and major elemental distribution in a 55 kyr peat deposit in tropical Australia: Implications to paleoclimate. *Geochimica et Cosmochimica Acta*. 72. pp. 449-463
- O'Leary, M. (1988): Carbon isotopes in photosynthesis. *Bioscience*. 38. 5. pp. 328-336
- Poto, L., Gabriel, J., Crowhurst, S., Agnostinelli, C., Spolaor, A., Cairns, W., Cozzi, G. & Barbante, C. (2015): Cross calibration between XRF and ICP-MS for high spatial resolution analysis of ombrotrophic peat cores for paleoclimatic studies. *Analytical and Bioanalytical Chemistry*. 407. pp. 379-385
- Reimer, P.J., Bard, E., Bayliss, A., Beck, J.W., Blackwell, P.G., Bronk Ramsey, C., Buck, C. E., Edwards, R. L., Friedrich, M., Grootes, P. M., Guilderson, T. P., Halfidson, H., Hajdas, I. Hatté, C., Heaton, T. J., Hoffman, D. L., Hogg, A. G., Hughen, K. A., Kaiser, K. F., Kromer, B., Manning, S. W., Niu, M., Reimer, R. W., Richards, D.A., Scott, E. M., Southon, J. R., Turney, C. S. M. & van der Plicht, J. (2013): IntCal13 and Marine 13 radiocarbon age calibration curves. 0-50.000 years cal BP. *Radiocarbon*. 55. pp.1869-1887
- Rydberg, J. (2014): Wavelength dispersive X-ray fluorescence spectroscopy as a fast. non-destructive and cost effective analytical method for determining the geochemical composition of small loose-powder sediment samples. *Journal of Paleolimnology*. 52 (3). pp. 265-276
- Sernander, R. (1908): On the evidences of Postglacial changes of climate furnished by the peat-mosses of Northern Europe. *Geologiska Föreningen i Stockholm Förhandlingar*. 30:7. pp. 465-473
- Shao, Y., Wyrwoll, K-H., Chappell, A., Huang, J., Lin, Z., McTinish, G., Mikami, M., Tanaka, T., Wang, X. & Yoon, S. (2011): Dust cycle: an emerging core theme in Earth system science. *Aeolian Research*. 2. pp. 181-204
- Svennson, G. (1988): Bog development and environmental-conditions as shown by the stratigraphy of Store Mosse mire in southern Sweden. *Journal of Ecology*. 76. pp. 41-59
- Tolonen, K. (1984): Interpretation of changes in the ash content of ombrotrophic peat layers. *Bulletin of the Geological Society of Finland*. 2. pp. 207-220

Weiss, D., Shotyk, W., Rieley, J., Page, S., Gloor, M., Reese, S. and Martinez-Cortizas, A. (2002): The geochemistry of major and selected trace elements in a forested peat bog, Kalimantan, SE Asia, and its implications for past atmospheric dust deposition. *Geochimica et Cosmochimica Acta*. 66. 13. pp. 2307-2323